Tailored surface energy of stainless steel plate coupons to reduce the adhesion of aluminium silicate deposit

Matjie, Ratale; Zhang, Shuai; Zhao, Qi; Mabuza, Nhlanganiso; Bunt, John R.

Published in:
Fuel

DOI:
10.1016/j.fuel.2016.04.105

Publication date:
2016

Tailored Surface Energy of Stainless Steel Plate Coupons to Reduce the Adhesion of Aluminium Silicate Deposit

Ratale Matjie[1*], Shuai Zhang[2], Qi Zhao[2*], Nhlanganiso Mabuza[3], John R Bunt[1]

[1]School of Chemical and Minerals Engineering, North-West University, Potchefstroom 2531, South Africa.

[2]School of Science and Engineering, University of Dundee, Dundee, DD1 4HN, UK

[3]Sasol Group Technology, Research and Technology, 1 Klasie Havenga Road, Sasolburg 1947, South Africa

* Corresponding authors: matjie4@gmail.com; q.zhao@dundee.ac.uk (Q.Zhao)

Abstract

Fouling in heat exchangers not only reduces heat transfer performance significantly, but also causes considerable pressure drop, resulting in higher pumping requirements. It would be much more desirable if surfaces which are inherently less prone towards fouling could be developed. In this paper, autocatalytic Nickel-Phosphorus-Polytetrafluoroethylene (Ni–P–PTFE) composite coatings and modified diamond-like carbon (DLC) coatings were applied to the coupons of the 316L stainless steel plates.

The effects of surface energies of the coatings on the adhesion of aluminium silicate fouling were investigated and the best surface energy for which the fouling adhesion is lowest was obtained. The experimental results show that the coating with the most favourable surface energy reduced the adhesion of aluminium silicate deposit by 97%, compared with uncoated stainless steel plate coupons. The anti-fouling mechanism of the coatings was explained with the extended Deryagin, Landau, Verwey and Overbeek (DLVO) theory.

Keywords: Fouling; Aluminium silicate; Stainless steel; Ni-P-PTFE coating; DLC coating; Surface energy.

1. Introduction

Heat exchangers are broadly applied in chemical industries to transfer thermal energy between different fluids. However, due to the properties of the different fluids, heat exchangers are usually prone to fouling on the metal surfaces. Fouling not only reduces heat transfer performance significantly, but also causes considerable pressure drop, calling for higher pumping requirements [1]. For example, experimental results have shown that a colloidal aluminium silicate precipitate can readily form on heat exchanger plates due to the presence of the aluminium, calcium, silicon, and iron species dissolved in the plant water during the gasification of coal using a commercial Fixed-Bed Dry-Bottom (FBDB) gasification technology [2]. The plant water typically contains 11-18ppm Si, 2-5ppm Al, 1-9ppm Ca, 0.1-5ppm Fe, 4-15 ppm Na, and 0.2-0.4% phenols with trace concentrations of K and P [2]. The formation of this gelatinous precipitate can result in

severe blockages of the heat exchanger plates and will eventually require unblocking with a toxic and highly corrosive inorganic acid. The formed gelatinous precipitate or deposit on the heat exchanger plates contains 71.3% SiO_2, 26.8% Al_2O_3, 0.6% Fe_2O_3, 0.03% TiO_2, 0.01% P_2O_5, 0.12% CaO, 0.69% MgO, 0.23% Na_2O and 0.17% K_2O [2].

It would be much more desirable if surfaces with an inherently lower affinity towards fouling could be developed. Many attempts have been made to reduce fouling by coating surfaces with Polytetrafluoroethylene (PTFE) due to its non-stickiness properties. However, the poor thermal conductivity, poor abrasion resistance, poor adhesion to metal substrate and industrial process conditions currently inhibit their commercial use [1]. The first electroless Ni–P–PTFE composite coatings were introduced about 30 years ago [3]. The incorporation of PTFE nanoparticles into the Ni–P matrix can take advantage of the different properties of Ni–P alloy and PTFE. The resulting properties of electroless Ni–P–PTFE coatings, such as non-stick property, higher dry lubricity, lower friction, good wear and good corrosion resistance, have been used successfully in many industries [1]. Because the electroless Ni–P–PTFE coatings are metal-based, their thermal conductivity, anti-abrasive property, mechanical strength and adhesion strength to the substrate are superior to standard PTFE coatings [1]. Zhao et al. demonstrated that the Ni-P-PTFE coatings effectively reduce the formation of bacteria and biofilms [3,4,5], crystalline deposit [1, 6] and food deposit [7]. Diamond-like carbon (DLC) coatings have attracted great interest due to their excellent properties such as excellent thermal conductivity similar to metals, low friction, extremely smooth surface, hardness, wear resistance and corrosion resistance [8]. The incorporation of selective elements into DLC has been shown to be an effective method to inhibit fouling

formation. Zhao et al. showed that the doped DLC coatings with Si, F or N reduce bacterial attachment [9,10] and crystalline deposit [11]. Ishihara et al. [12] also demonstrated that the antibacterial performance of the pure DLC coatings was improved significantly by the incorporation of fluorine with *Escherichia coli*. However, to date no research has been reported for the use of Ni-P-PTFE coatings or DLC coatings to reduce aluminium silicate fouling. In this paper, autocatalytic Ni–P–PTFE composite coatings and modified diamond-like carbon (DLC) coatings were applied to stainless steel plates and the effects of surface energies of the coatings on the adhesion of aluminium silicate fouling were investigated at the South African solvent extraction plants.

2. Experimental Procedure

2.1. Ni–P–PTFE composite coatings

Ni–P–PTFE coating was prepared on 2B stainless steel 316 heat exchanger plate coupons (200mm length X 100mm width X 0.6mm thickness) using an electroless plating technique. The stainless steel plate coupons were first cleaned with an alkaline solution at 60–80°C for 10–20 min and then rinsed with deionised water. The composition of the alkaline solution included 25 g/l NaOH; 30 g/l Na_3PO_4; 25 g/l Na_2CO_3 and 5 g/l Na_2SiO_3. The plate coupons were dipped into a dilute hydrochloric solution (1 M) for 30 seconds and then rinsed with cold water and deionized water, respectively. A 60% PTFE emulsion with a particle size in the range 0.05–0.5 μm was diluted with

deionized water and stirred with a magnetic stirrer for 1 h. The solution was then filtered with a filter of pore size 0.2 μm before use. The composition of electroless Ni–P–PTFE solutions used in this investigation included 50 g/l $NiSO_4 \cdot 6H_2O$; 60 g/l $Na_3C_6H_5O_7 \cdot 2H_2O$; 25 g/l $NaH_2PO_2 \cdot H_2O$; 40 g/l NH_4CH_3COO; 4–18 ml/l PTFE (60 wt %) and 0–0.6 g/l cationic surfactant. The PTFE contents in the coatings were altered by changing the concentration of PTFE emulsion in the plating bath. The coating thickness was measured using a digital micrometer and the coating compositions were analysed with an energy dispersive X-ray microanalysis (EDX) at a beam energy of 20 keV. The surface morphology of the coatings was analysed with a scanning electron microscope (SEM). The thickness of the doped Ni-P-PTFE coating was about 10 μm, which was controlled by the deposition time. Two types of Ni-P-PTFE coatings with 4.0 wt% PTFE and 5.1 wt% PTFE were prepared.

2.2. Doped DLC coatings

The doped DLC coatings with N, Si and F were prepared on stainless steel 316 stainless steel plate coupons by plasma-enhanced chemical vapour deposition technique. The stainless steel plate coupons were cleaned in an ultrasonic bath containing acetone for 10 min, rinsed with distilled water and dried before coating. The substrates were further cleaned by Ar+ bombardment prior to deposition. Acetylene was used as the process gas for the DLC coating. The N-doped, Si-doped and F-doped DLC coatings were produced by introducing nitrogen, tetramethylsilane and tetrafluoromethane, respectively. The N, Si or F contents in the DLC coatings were altered by changing the gas flow rate of nitrogen, tetramethylsilane or

tetrafluoromethane, respectively in the range between 0 sccm and 10 sccm (standard cubic centimetres per minute). The thickness of the doped DLC coatings was about 1 μm, which was controlled by the deposition time. The N, Si or F content in the DLC coatings was analyzed by EDX. The doped DLC coatings with 1.6% N, 4.1% N, 8.1% N, 7.0% Si, 5% F and 15% F were prepared. Standard DLC coatings were also prepared as a control.

2.3. Contact angle measurements

Prior to contact angle measurement, the coatings were ultrasonically cleaned in acetone, ethanol and deionized water in sequence. Contact angles were obtained using the sessile drop method with a Data physics OCA-20 contact angle analyser with an accuracy of ± 0.1 °. Three test liquids were used as a probe for surface free energy calculations: distilled water, di-iodomethane and ethylene glycol. The data for surface tension components of the test liquids are given in Table 1 [13]. 6 measurements per test liquid were performed to determine the contact angles and the mean contact angles and the corresponding standard deviation were given in Table 2. The contact angles of an untreated coupon of stainless steel plate and aluminium silicate deposit were also measured. All measurements were made at 25 °C.

2.4. Surface free energy

The theory of the contact angle of pure liquids on a solid substrate was developed

200 years ago in terms of the Young equation [14]:

$$\gamma_L \cos\theta = \gamma_S - \gamma_{SL} \quad (1)$$

where γ_L is the experimentally determined surface tension of the liquid; θ is the contact angle; γ_S is the surface free energy of the solid and γ_{SL} is the solid/liquid interfacial energy. In order to obtain the solid surface energy γ_S, an estimate of γ_{SL} has to be obtained. Van Oss et al [15] developed an acid-base approach for the calculation of surface energy. The surface energy is seen as the sum of a Lifshitz-van der Waals apolar component γ_i^{LW} and a Lewis acid-base polar component γ_i^{AB}:

$$\gamma_i = \gamma_i^{LW} + \gamma_i^{AB} \quad (2)$$

The acid-base polar component γ_i^{AB} can be further subdivided by using specific terms for an electron donor (γ_i^-) and an electron acceptor (γ_i^+) subcomponent:

$$\gamma_i^{AB} = 2\sqrt{\gamma_i^+ \gamma_i^-} \quad (3)$$

The solid/liquid interfacial energy is then given by:

$$\gamma_{SL} = \gamma_S + \gamma_L - 2(\sqrt{\gamma_S^{LW} \cdot \gamma_L^{LW}} + \sqrt{\gamma_S^+ \cdot \gamma_L^-} + \sqrt{\gamma_S^- \cdot \gamma_L^+}) \quad (4)$$

Table 1 Test liquids and their surface tension components [13]

Surface tension data (mN/m)	γ_L	γ_L^{LW}	γ_L^{AB}	γ_L^+	γ_L^-
Water (W), H_2O	72.8	21.8	51.0	25.5	25.5
Diiodomethane (D), CH_2I_2	50.8	50.8	0	0	0
Ethylene glycol (E), $C_2H_6O_2$	48.0	29.0	19.0	1.92	47.0

Table 2 Contact angle and surface energy components of coatings

Coatings		**Contact Angle θ [°]**			**Surface Energy Components [mJ/m²]**				
Name	**Chemistry**	θ^W	θ^{Di}	θ^{EG}	γ^{LW}	γ^+	γ^-	γ^{AB}	γ^{TOT}
1	Ni-P-PTFE (4.0% PTFE)	85.1±2.4	64.2±0.6	70.6±0.6	26.16	0.00	9.42	0.16	26.32
2	Ni-P-PTFE (5.1% PTFE)	84.5±0.7	70.1±0.9	75.2±0.7	22.82	0.01	11.60	0.52	23.34
3	DLC coating	79.9±0.8	49.6±0.7	59.4±0.6	34.49	0.00	8.84	0.40	34.90
4	N-DLC (1.6% N)	90.0±0.9	49.3±0.3	60.2±0.6	34.66	0.11	2.07	0.93	35.60
5	N-DLC (4.1% N)	85.8±0.9	44.5±0.3	59.2±0.6	37.28	0.01	3.99	0.37	37.65
6	N-DLC (8.1% N)	77.3±0.7	43.2±0.6	47.0±0.5	37.96	0.28	6.58	2.71	40.68
7	Si-DLC (7.0% Si)	85.9±0.7	50.0±0.4	63.8±0.6	34.27	0.00	5.22	0.11	34.38
8	F-DLC (5% F)	82.5±0.3	59.6±0.3	57.4±0.4	28.80	0.44	6.38	3.33	32.14
9	F-DLC (15% F)	90.5±0.9	61.2±1.3	71.4±2.0	27.88	0.00	5.05	0.07	27.95
10	Stainless steel (untreated)	69.4±1.1	35.6±0.3	47.1±0.9	41.75	0.09	6.19	1.52	43.27
11	Aluminium silicate deposit	102.5±3.0	0	74.0±0.9	50.80	1.39	4.51	5.02	55.82

Combining this with the Young equation (1), a relation between the measured contact angle and the solid and liquid surface free energy terms can be obtained:

$$\gamma_L \cdot (1+\cos\theta) = 2(\sqrt{\gamma_S^{LW} \cdot \gamma_L^{LW}} + \sqrt{\gamma_S^{+} \cdot \gamma_L^{-}} + \sqrt{\gamma_S^{-} \cdot \gamma_L^{+}}) \quad (5)$$

In order to determine the surface free energy components (γ_S^{LW}) and parameters γ_S^{+} and γ_S^{-} of a solid, the contact angles of at least three liquids with known surface tension components ($\gamma_L^{LW}, \gamma_L^{+}, \gamma_L^{-}$), two of which must be polar, have to be determined.

2.5. Experiments of aluminium silicate fouling

Stainless steel coupons (200mm length X 100mm width X 0.6mm thickness) were cut from a new heat exchanger stainless plate (371mm×871mm×0.6mm) for coating with Ni–P–PTFE and DLC. The coated plate coupons were attached to the flange on the inside of process pipes connecting the extractors and the heat exchangers and subsequently evaluated in the South African solvent extraction plants over a period of ten months for the deposition of colloidal aluminium silicate. An untreated stainless steel plate coupon was also evaluated as the control. The flange with the attached coated and uncoated stainless steel coupons was installed in the process pipe connected to the heat exchangers and the coupons were tested at 55-72°C in the hot plant water containing Al, Si, Fe and Ca ions and phenolics. A significant amount of the colloidal aluminium silicate deposit was formed on the internal walls of the plant process pipe when the plant water was flowing through this pipe. High temperatures of the plant

water could result in significant amount of aluminium silicate precipitate formed in the plant equipment. The pH and the flow rate of hot plant water flowing through the process pipe were 8.8 and 760m^3/h respectively. After treating the coated and uncoated plate coupons with hot plant water for 5 months using above mentioned experimental conditions, the tested coupons attached to the flange were subsequently removed from the process pipe for the visual observations. The observed tested coupons attached to the flange were reinstalled in the same process pipe and the coupons were subsequently re-exposed to hot plant water containing Al ions, Si ions, Ca ions, Fe ions and phenols for further 5 months. The total experimental period was 10 months. 3 other uncoated coupons had been previously tested at identical conditions, which were completely covered by aluminium silicate deposit after the experiments and there was no significant difference between them on the average coverage and weight of fouling deposits.

3. Experimental Results

3.1. Surface characterization

Figure 1(a) shows a typical SEM image of Ni-P-PTFE coating with 5.1 wt% PTFE, which shows that the PTFE particles were homogenously distributed in the Ni-P matrix. The element compositions of the Ni–P–PTFE coating were determined by EDX analysis (Figure 1b) and the PTFE content was calculated based on the fluorine content in the coating. The N, Si or F content in the DLC coatings was analyzed by EDX. Figures 2(a) and 2(b) show typical EDX images of N-doped DLC coating (8.1% N) and Si-doped DLC

coating (7.0% Si), respectively. The detailed chemical compositions of the Ni-P-PTFE coatings and the doped DLC coatings are given in Table 2.

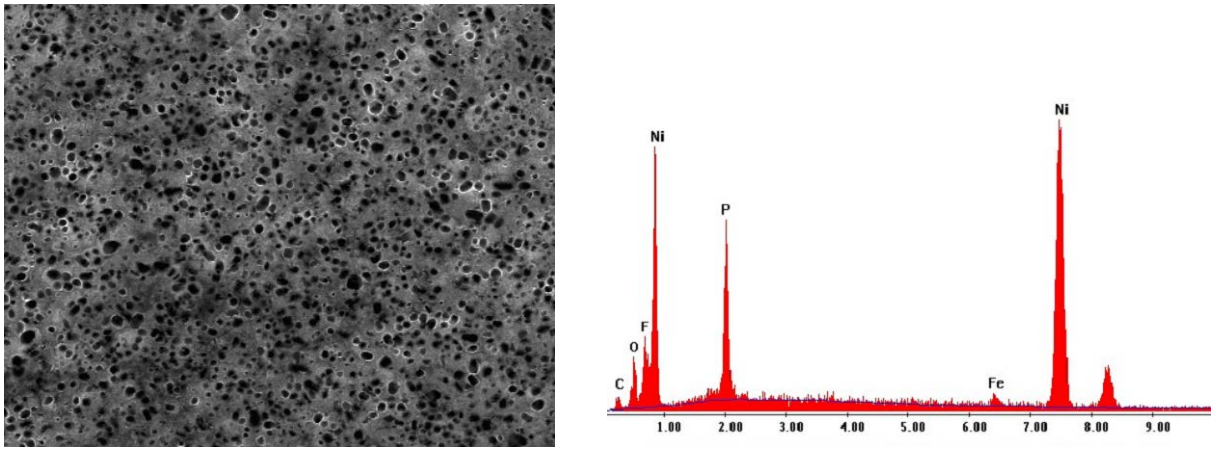

(a) (b)

Figure 1 (a) SEM image of Ni-P-PTFE; (b) EDX image of Ni-P-PTFE

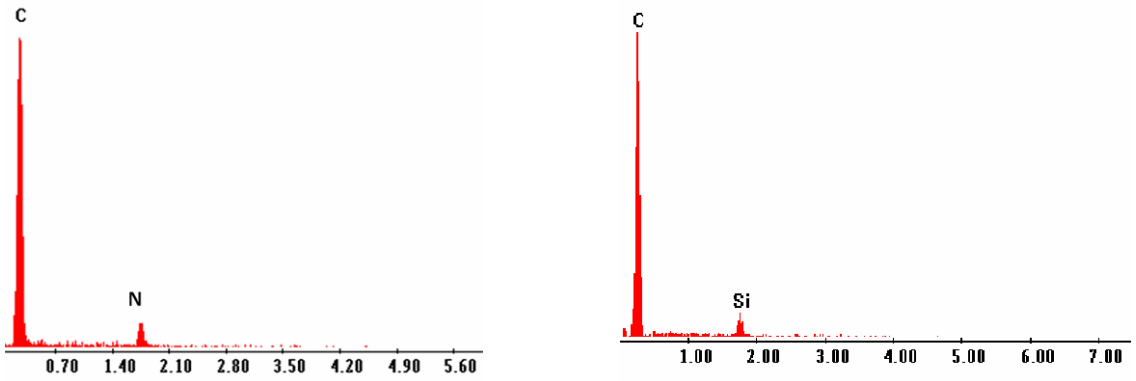

(a) (b)

Figure 2 (a) EDX image of N-doped DLC with 8.1% N; (b) EDX image of Si-doped DLC with 7.0% Si

3.2 Contact angle and surface energy component

Table 2 shows the contact angle and surface energy of the Ni-P-PTFE coatings and the doped DLC coatings used in this investigation. Table 2 also shows the contact angle and surface energy of aluminium silicate deposit. For the Ni-P-PTFE coatings, surface energy decreases with PTFE content increasing. For N-doped DLC coatings, the surface energy increases with N content increasing. For F-doped DLC coatings, the surface energy decreases with F content increasing. The surface energy of the untreated stainless steel plate coupon was 43 mJ/m^2, which was higher than those of the coatings. The surface energy of the coatings was in the range of 23.34 – 40.68 mJ/m^2. The surface energy of the aluminium silicate deposit was very high, about 56 mJ/m^2.

3.3. Aluminium silicate fouling

It was visually observed that the uncoated coupons of the heat exchanger plate were fully covered by the aluminium silicate deposit after testing these coupons in the process pipe for 5 months, whilst the coated plate coupons were not covered by the aluminium silicate deposit. The experimental results also showed that the untreated stainless steel plate coupons were fully covered with the aluminium silicate fouling deposit after testing the coupons for 10 months. The deposit strongly adhered to the surface and was difficult to remove. The two Ni-P-PTFE coated plate coupons were also fully covered with fouling deposits. However the wet deposit was loosely adhered and could be removed easily. All the doped DLC coatings showed excellent anti-fouling properties.

Most of the coated surfaces were clean (without fouling deposits) and only a few parts were covered with scattered fouling particles after testing the coupons for 10 months. The wet deposits were very loosely adhered and very easily to be removed by water.

The fouling deposit was dried and removed from each coupon surface. Then it was weighed using a Sartorius electronic scale with 10^{-5} g precision. The mass of the deposit was divided by the projected area of the plate coupon to calculate deposit surface density in mg/cm^2: For the untreated stainless steel plate coupon, it was 26.77 mg/cm^2; for the Ni-P-PTFE coated plate coupon, it was 21.83 - 24.08 mg/cm^2; while for the doped DLC coated plate coupon, it was in the range of 0.7 – 6.10 mg/cm^2. Figure 3 shows the effect of surface energy on the adhesion of aluminium silicate fouling. Clearly there exists the most favourable surface energy of the coatings (about 35 mJ/m^2), at which the adhesion of aluminium silicate fouling was lowest. The N-doped DLC coating (1.6% N) performed best in inhibiting fouling formation, which reduced fouling formation by 97% compared with untreated stainless steel plate coupons.

Figures 4a and 4b show typical aluminium silicate fouling patterns on untreated stainless steel coupon with surface energy of 43.27 mJ/m^2 and on N-DLC coated coupon with surface energy of 35.6 mJ/m^2, respectively. Clearly the untreated stainless steel plate coupons were fully covered with the aluminium silicate fouling deposit after 5 months; while only a few parts of the N-DLC coating were covered with thin scattered fouling particles after 10 months.

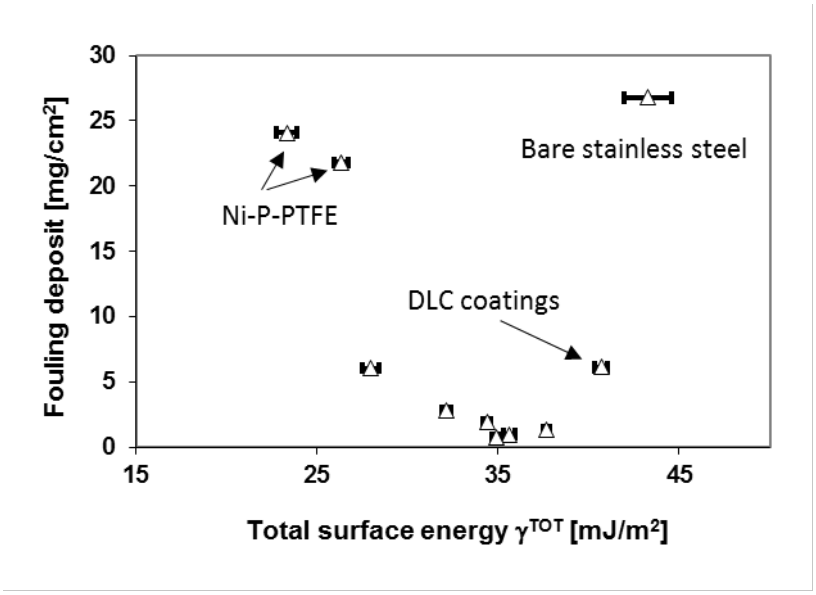

Figure 3 Effect of total surface energy on the adhesion of aluminium silicate fouling (Bare stainless steel and Ni-P-PTFE coatings were fully coved with the deposit; while the DLC coatings were only partially coved with the deposit)

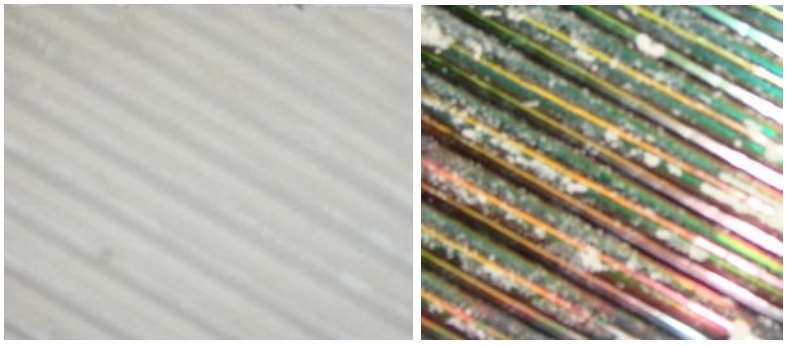

(a) (b)

Figure 4 Aluminium silicate fouling formation on (a) untreated stainless steel coupon with surface energy of 43.27 mJ/m^2 and (b) N-DLC coated coupon with surface energy of 35.6 mJ/m^2.

4. Discussion: adhesion mechanism

Particulate fouling adhesion may be described with the extended DLVO (Deryagin, Landau, Verwey and Overbeek) theory [16]. According to this theory, the principal interaction forces determining hetero-coagulation include a Lifshitz-van der Waals (LW) interaction component, an electrostatic double-layer (EL) component, a Lewis acid-base (AB) component, and Brownian motion (Br). The total interaction energy ΔE_{132}^{TOT} between particulate (1) and a solid surface (2) in a fluid (3) can be written as the sum of these corresponding interaction terms [16]:

$$\Delta E_{132}^{TOT} = \Delta E_{132}^{LW} + \Delta E_{132}^{AB} + \Delta E_{132}^{EL} + \Delta E_{132}^{Br} \quad (6)$$

The balance between all possible interactions determines whether or not the particulate will attach on the surface: adhesion will take place when ΔE_{132}^{TOT} is negative (i.e. total interaction force is attractive).

Zhao and Müller-Steinhagen [1] derived the optimum surface energy components of a surface, for which particulate adhesion force is minimal, using the extended DLVO theory:

$$\gamma_S^{TOT} = \frac{1}{4} \cdot (\sqrt{\gamma_1^{LW}} + \sqrt{\gamma_3^{LW}})^2 \quad (7)$$

where γ_S^{TOT} , γ_1^{LW} and γ_3^{LW} are the surface free energy of the surface (e.g. coating), particles (e.g. aluminium silicate) and fluid (e.g. water) respectively. They can be determined experimentally. As the equation isolates the effect of surface energy upon particulate adhesion from the numerous parameters in the extended DLVO theory, it appears relatively simple.

Equation (7) explains the experimental results in Figure 3 – while aluminium silicate adhesion was lowest when the surface energy of the coatings was about 35 mJ/m^2. The γ_1^{LW} value of aluminium silicate is 50.8 mJ/m^2 (see Table 1) and γ_3^{LW} of water is 21.8 mJ/m^2 (see Table 2). Equation (7) then produces a theoretical value of γ_S^{TOT} =34.8 mJ/m^2, which approximates the experimental value of the surface energy for which aluminium silicate adhesion was lowest.

In addition to surface energy, other factors, including zeta potentials, surface roughness, temperature and fluid flow velocity also have a significant influence on aluminium silicate adhesion [17]. It was reported that the zeta potential of DLC coatings are -35 mv [18] and the zeta potential of Ni-P-PTFE coatings and bare stainless steel are around -25 mv [4]; while the zeta potential of aluminium silicate is -44 mV [19]. As the DLC coatings are more negatively charged compared with stainless steel, the DLC coatings are more repellent to the negatively charged aluminium silicate. The mechanisms of aluminium silicate adhesion are complex. If, however, initial aluminium silicate adhesion strength is reduced by the best surface energy approach, they could be removed easily from the surfaces by flowing water. This may lead to a way of

controlling particulate fouling formation.

5. Conclusions

In this paper, autocatalytic Ni–P–PTFE composite coatings and modified diamond-like carbon (DLC) coatings were applied to coupons of the stainless steel heat exchanger plates. The experimental results demonstrate that the surface energies of the coatings have a significant influence on the adhesion of aluminium silicate fouling. When the surface energy of the coatings was about 35 mJ/m^2, the aluminium silicate adhesion was lowest. The experimental results also show that the coating with the surface energy reduced the adhesion of aluminium silicate deposit by 97%, compared with uncoated coupons of the stainless steel heat exchanger plate. The anti-fouling mechanism of the coatings was successfully explained with the extended DLVO theory.

Acknowledgment

This paper was developed from a collaborative research program between Sasol Synfuels; Sasol Technology Research & Development (R&D) and the Department of Mechanical Engineering at the University of Dundee. The support provided by the Sasol Maintenance Foreman and his team is gratefully acknowledged. The information presented in this paper is based on the research financially supported by the South African Research Chairs Initiative (SARChI) of the Department of Science and Technology and National Research Foundation of South Africa (Coal Research Chair

Grant No. 86880). Any opinion, finding or conclusion or recommendation expressed in this material is that of the author(s) and the NRF does not accept any liability in this regard.

References

[1] Q. Zhao, Y. Liu, S. Wang, H. Müller-Steinhagen. Chem. Eng. Sci. 60 (17) (2005) 4858.

[2] R.H. Matjie and R. Engelbrecht. Hydrometallurgy. 2007:85:172-182.

[3] S.S. Tulsi. Finishing 7 (1883)14.

[4] C. Liu, Q. Zhao, Biofouling 27 (3) (2011) 275.

[5] Q. Zhao, Y. Liu, J. Food Eng. 72 (3) (2006) 266.

[6] Q. Zhao, Y. Liu, S. Wang. Desalination 180 (1-3) (2005) 133.

[7] W. Liu, P.J. Fryer, Z. Zhang, Q. Zhao, Y. Liu. Innov Food Sci Emerg 7 (4) (2006) 263.

[8] A. Grill, Wear 168 (1993) 143.

[9] Q. Zhao, X.J. Su, S. Wang, X. Zhang, P. Navabpour, D. Teer, Biofouling 25 (2009) 377.

[10] Q. Zhao, X. Wang, Surf Coat Tech 192 (2005) 77.

[11] H. Müller-Steinhagen, Q. Zhao, A. Helali-Zadeh, X. Ren, Can J Chem Eng 78 (2000) 12.

[12] M. Ishihara, T. Kosaka, T. Nakamura, K. Tsugawa, M. Hasegawa, F. Kokai, Y. Koga, Diam Relat Mater 15 (2006) 1011.

[13] C.J. van Oss, L. Ju, M.K. Chaudhury, R.J. Good. J Colloid Interface Sci 128 (1989) 313.

[14] T. Young. Philosophical Transactions of the Royal Society London 95 (1805) 65.

[15] C.J. van Oss, M.K. Chaudhury. Langmuir 4 (1988) 884.

[16] C.J. van Oss, Interfacial Forces in Aqueous Media. Marcel Dekker, New York, 1994.

[17] H. Muller-Steinhagen, M. Jamialahmadi, Understanding Heat Exchanger Fouling And Its Mitigation 1 (1999) 209.

[18] E. Salgueiredo, M. Vila, M.A. Silva, M.A. Lopes, J.D. Santos, F.M. Costa, R.F. Silva, P.S. Gomes, M.H. Femandes. Diamond and Related Materials 17(2008) 878.

[19] T. Yokoyama, A. Ueda, K. Kato, K. Mogi, S. Matsuo. Journal of Colloid and Interface Science 252 (2002) 1.